

SO(4), SO(3) and SU(2) gauge theories in 2+1 dimensions: comparing glueball spectra and string tensions

Michael Teper

Rudolf Peierls Centre for Theoretical Physics, University of Oxford,
1 Keble Road, Oxford OX1 3NP, UK

and

All Souls College, University of Oxford,
High Street, Oxford OX1 4AL, UK

Abstract

We improve upon recent calculations of the low-lying ‘glueball’ spectra of $SO(3)$ and $SO(4)$ lattice gauge theories in 2+1 dimensions, and compare the resulting continuum extrapolations with $SU(2)$. We find that these are reasonably consistent, as are the $SU(2)$ and $SO(4)$ string tensions when these are corrected for the differing representations of the flux. All this indicates that the different global properties of these groups do not play a significant role in the low-lying physics.

E-mail: mike.teper@physics.ox.ac.uk

Contents

1	Introduction	1
2	Lattice preliminaries	1
3	SO(4) and SU(2)×SU(2)	4
4	SO(3) and SU(2)	5
5	Conclusions	6

1 Introduction

Certain $SU(N)$ and $SO(N')$ groups share the same Lie algebra, although their global structure differs: that is to say, $SO(3)$ and $SU(2)$, $SO(4)$ and $SU(2) \times SU(2)$, $SO(6)$ and $SU(4)$. It is interesting to ask which if any of the physical properties of the corresponding gauge theories are sensitive to these global differences. A recent paper [1] has addressed this question for the lightest glueball masses and the string tension in the context of a calculation of $SO(N)$ gauge theories for all N . Unfortunately most of the masses calculated in $SO(N)$ at small values of N turned out to be subject to large systematic errors, making the desired comparison of limited value. In this paper we will improve substantially upon the $SO(4)$ calculations, and significantly upon the $SO(3)$ ones, allowing us to make a more useful comparison than that provided in [1]. Since the calculations in [1] were for gauge theories in $2 + 1$ dimensions, so are the calculations in the present paper.

Since this work represents a direct continuation of (some of) the work in [1] we will not repeat the discussion in that paper and will simply focus on the way that our calculations differ. For a detailed discussion of methods etc. we direct the reader to [1].

As an aside we remark that another paper [2] has compared the deconfining temperature in $SO(4)$ and $SO(6)$ gauge theories against existing calculations for $SU(2)$ and $SU(4)$ respectively. The continuum values, expressed in units of the string tension and corrected for the differing representations, agree within two standard deviations.

2 Lattice preliminaries

We replace continuum (Euclidean) space-time by a cubic lattice with a lattice spacing labelled by a . The lattice is of finite size, $L_x \times L_y \times L_t$ in lattice units, with periodic boundary conditions. The variables are $N \times N$ $SO(N)$ matrices, U_l , living on the lattice links l that join neighbouring sites. The Euclidean path integral is $Z = \int \mathcal{D}U \exp\{-S[U]\}$ where $\mathcal{D}U$ is the Haar measure. We use the standard plaquette action,

$$S = \beta \sum_p \left\{ 1 - \frac{1}{N} \text{Tr} U_p \right\} \quad ; \quad \beta = \frac{2N}{ag^2} \quad (1)$$

where U_p is the ordered product of link matrices around the plaquette p . As a convenient shorthand, we shall use $u_p \equiv \frac{1}{N} \text{Tr} U_p$. We have written $\beta = 2N/ag^2$, but strictly speaking this ag^2 is just one possible definition of the dimensionless coupling on the length scale a . So if we were to be more precise we would write $\beta = 2N/ag_p^2$ with $ag_p^2 \stackrel{a \rightarrow 0}{\equiv} ag^2 + ca^2g^4 + \dots \stackrel{a \rightarrow 0}{\rightarrow} ag^2$ where g^2 is the coupling in the continuum limit.

The purpose of the lattice calculations is to calculate the physics of the corresponding continuum gauge theories. Since ag^2 , the dimensionless running coupling on the scale of the lattice spacing, vanishes as $a \rightarrow 0$ one can determine the leading lattice corrections just as one does for asymptotically free gauge theories in 3 + 1 dimensions. So we know that ratios of two physical masses satisfy

$$\left. \frac{am_1}{am_2} \right|_a \equiv \left. \frac{m_1}{m_2} \right|_a \stackrel{a \rightarrow 0}{\equiv} \left. \frac{m_1}{m_2} \right|_{a=0} + c(am_3)^2 + O(a^4) \quad (2)$$

where am_3 is some other mass (which may equal am_1 or am_2) and c is some constant (that depends of course on m_1, m_2, m_3). We can then use this to extrapolate our results to the continuum limit. We can also extrapolate a lattice mass am expressed in units of a lattice coupling ag^2 using

$$\left. \frac{am}{ag^2} \right|_a = \left. \frac{m}{g^2} \right|_a \stackrel{a \rightarrow 0}{\equiv} \left. \frac{m}{g^2} \right|_{a=0} + cag^2 + O(a^2). \quad (3)$$

Here the leading correction is $O(a)$ rather than $O(a^2)$ because the running dimensionless coupling is not a physical quantity even though the continuum coupling is. The most straightforward definition of a coupling is $\beta = 2N/ag^2$ as in eqn(1). However we prefer to use the mean-field improved coupling

$$\beta_I = \beta \langle u_p \rangle \equiv \frac{2N}{ag_I^2} \quad (4)$$

since there are some theoretical arguments [3] that the lattice corrections are smaller using this coupling, as appears to be borne out in practice for $SU(N)$ gauge theories [4].

The energy of a state can be calculated from the time dependence of a correlation function

$$\langle \phi^\dagger(t) \phi(0) \rangle = \sum_n |\langle \text{vac} | \phi^\dagger | n \rangle|^2 e^{-E_n t} \stackrel{t \rightarrow \infty}{\propto} e^{-Mt} \quad (5)$$

where M is the mass of the lightest state with the quantum numbers of the operator ϕ . The operator ϕ will typically be the trace of the product of $SO(N)$ link matrices around some closed path. To have good overlaps onto the desired states, so that one can evaluate masses at values of t where the signal has not yet disappeared into the statistical noise, one needs to use blocked and smeared operators. (For more details see [1].) This method can be generalised to a variational calculation over a basis of operators, thus allowing for the efficient calculation of the energies of excited states [1]. The blocking/smearing involves a parameter that determines the weighting of the direct path between two sites and the ‘staples’ that constitute the smearing. In the $SO(N)$ calculations of [1] one used the same value for this smearing parameter as the one that had previously been used in $SU(N)$ calculations [5, 6].

In this paper we have attempted to optimise the value of this parameter for $SO(3)$, $SO(4)$ and $SO(6)$ by performing calculations with various values of the parameter. We find that for $SO(3)$ the best parameter should be chosen to be about 2.5 times the value used in [1] and for $SO(4)$ about 1.7 times. For $SO(6)$ we find there is much less to be gained and for that reason we do not attempt to redo the $SO(6)$ calculations in this paper.

To illustrate the improvement we obtain with our operators in this paper, it is useful to define an effective mass $M_{eff}(t)$ by

$$\frac{\langle \Psi^\dagger(t+a)\Psi(0) \rangle}{\langle \Psi^\dagger(t)\Psi(0) \rangle} = e^{-aM_{eff}(t)}. \quad (6)$$

Comparing eqn(5) and eqn(6) it is clear that what we want is for $M_{eff}(t)$ to approach its asymptotic value as quickly as possible as t increases, i.e. that the normalised overlap of our operator Ψ on the desired ground state should be as close to unity as possible. We display in Fig. 1 the effective masses for a sample of glueball states ranging from the lightest to the heaviest in one of our $SO(4)$ calculations. The operators used are the best variational operators using either the basis of this paper (solid points) or the basis (open points) of [1]. The horizontal lines are our best mass estimates obtained from the apparent large- t limits of the effective masses using the new operators. It is clear that for all the states, apart from the very lightest glueball, the new operators provide a much more credible estimate of the large- t plateau of $M_{eff}(t)$ which corresponds to the ground state mass. It is nonetheless also clear that even with these new operators identifying an effective mass plateau for the very heaviest states is significantly uncertain. Since the lattice used in Fig. 1 has the second smallest lattice spacing of our $SO(4)$ calculation, this caveat certainly applies to our eventual continuum extrapolations.

In Fig. 2 we provide a similar effective mass comparison for our $SO(3)$ calculation at the smallest lattice spacing. While the new calculation is clearly better than that in [1] the improvement is less striking than for $SO(4)$. The reason for this is presumably that for $SO(3)$ the only difference with the calculations of [1] is in the choice of the smearing parameter, while for $SO(4)$ the operator basis used in [1] was in addition significantly smaller. It is also clear from a comparison of Fig. 2 and Fig. 1 that the $SO(4)$ calculations have better overlaps than the $SO(3)$ ones and hence lead to more reliable mass estimates. This is something already noted in the study of $SO(N)$ gauge theories in [1]: as we increase N the overlaps improve. Indeed for $SO(6)$ we found that changing the smearing parameter did not lead to an improvement that was large enough to motivate a new calculation.

A calculation in [1] that helped elucidate the origins of the poor overlaps in $SO(3)$ was the comparison of the effective mass plots one obtains in $SU(2)$ using glueball operators where the trace of the closed loop is taken in the adjoint and fundamental representations respectively. One found [1] that using the adjoint in $SU(2)$ led to poor overlaps similar to those seen using the fundamental in $SO(3)$. Since these representations correspond to each other, this demonstrates that this problem is not peculiar to $SO(N)$ gauge theories. As an addendum to that we show in Fig. 3 a similar comparison for $SU(4)$, but this time using operators in the fundamental and $k = 2$ (antisymmetric) representations, since the latter corresponds to

the fundamental of $SO(6)$. We see that the overlaps of the $k = 2$ operators are visibly worse although the effect is modest except for the heaviest states. The $SO(6)$ overlaps are quite similar to this.

3 $SO(4)$ and $SU(2) \times SU(2)$

We begin with $SO(4)$ and $SU(2) \times SU(2)$. If the physics of these two gauge groups is the same then the physics of $SO(4)$ is just that of two non-interacting $SU(2)$ groups. That is to say, the single-particle mass spectrum of $SO(4)$ should be identical to that of $SU(2)$, and taking into account the differences in the fundamental representations, the string tensions should differ by a factor of two [1]

$$\sigma|_{so4} = 2 \sigma|_{su2} \quad (7)$$

and the couplings also by a factor of two [1]

$$g^2|_{so4} = 2 g_f^2|_{su2}. \quad (8)$$

We start with the string tension. In Table 1 we list our calculated masses of the flux loops winding around the spatial torus at various bare couplings. From these we can extract the listed values of the string tension, as explained in [1] and we can then extract a continuum value for $\sqrt{\sigma}/g^2$ with the fit

$$\left. \frac{\sqrt{\sigma}}{g_f^2 N} \right|_{so4} = 0.05889(41) - 0.00048(18) a g_f^2 N \quad , \quad \chi^2/n_{dof} = 1.39 \quad (9)$$

Taking the above continuum value of $\sqrt{\sigma}/g^2$ and imposing the relations eqns(7,8) we obtain a predicted value for $SU(2)$

$$\left. \frac{\sqrt{\sigma}}{g^2} \right|_{so4} = 0.2356(16) \implies \left. \frac{\sqrt{\sigma}}{g^2} \right|_{su2} = 0.3332(23). \quad (10)$$

This is to be compared to the directly calculated $SU(2)$ value of $\sqrt{\sigma}/g^2|_{su2} \simeq 0.3349(3)$, as given in Table B1 of [5]. These values are in agreement within errors. We can perform the same analysis for the mass gap using the values listed in Table 2. We obtain the continuum fit

$$\left. \frac{m_{0+}}{g_f^2 N} \right|_{so4} = 0.1957(25) - 0.00084(100) a g_f^2 N \quad , \quad \chi^2/n_{dof} = 0.48 \quad (11)$$

from which we obtain a prediction for $SU(2)$

$$\left. \frac{m_{0+}}{g^2} \right|_{so4} = 0.783(10) \implies \left. \frac{m_{0+}}{g^2} \right|_{su2} = 1.566(20). \quad (12)$$

This is to be compared to the directly calculated $SU(2)$ value of $m_{0+}/g^2|_{su2} \simeq 1.586(2)$, as given in Table B1 of [5]. These values are again in agreement within errors. Thus as far as

the mass gap and fundamental string tension are concerned $SO(4)$ is just like $SU(2) \times SU(2)$, at least within our percent level errors.

As an aside it is useful to look at the actual lattice data on a plot versus ag_7^2 . This we do for m_{0^+}/g^2 and $\sqrt{\sigma}/g^2$ in Fig. 4 where we also show our continuum extrapolations. We note that the best fits shown have very small slopes: that is to say, these dimensionless ratios are consistent with having almost no lattice corrections. On the other hand we can see in Fig. 4 that in units of ag^2 the range of our calculated values is not large, and in fact hardly larger than the range over which we need to extrapolate to the continuum. This is uncomfortable: a long extrapolation may conceal significant systematic errors. To avoid this we can instead look at physical mass ratios where the leading correction is $O(a^2\mu^2)$ (with μ some reasonable mass scale such as m_{0^+} or $\sqrt{\sigma}$) in which case our calculated values extend to a region much closer to the continuum limit, as we shall now see.

In Table 2 we list our best estimates for the masses of the same glueball states as calculated in [1]. As can be seen from the examples of effective masses in Fig.1 the heavier the glueball the less reliable is our estimate of its mass. We perform continuum extrapolations of the dimensionless ratio $m/\sqrt{\sigma}$ using the string tensions listed in Table 1. In general we obtain acceptable fits to our masses with just a lowest order $O(a^2\sigma)$ lattice correction and we use these fits to estimate the continuum mass ratios listed in Table 3, where we also give the χ^2 per degree of freedom of each fit. A selection of continuum extrapolations are shown in Fig. 5. Although the displayed best fits have small but non-zero slopes, in fact the slopes are consistent with zero within errors, i.e. consistent with negligible lattice corrections. This is in fact the case for our continuum fits to all the states in Table 3. Moreover here the range over which we have calculated masses extends much closer to the continuum limit, largely eliminating any worry about associated systematic errors.

In Table 3 we also list the corresponding mass ratios in $SU(2)$. We see that we have good agreement, within 1σ , between the $SO(4)$ and $SU(2)$ values for the $0^+, 0^{+*}, 2^-$ and 0^- glueballs, and acceptable agreement, i.e. within about 2σ , for all the rest except for the 2^+ , the 2^{-*} (both about 3σ) and the 1^+ (about 4σ). The fact that these larger discrepancies are all in one direction, i.e. the $SO(4)$ ratios larger than the $SU(2)$ ones, is consistent with the fact that for heavier states our identification of an effective mass plateau is weak, and by extracting a mass too early along the correlator we overestimate the mass. Nonetheless we see that the bulk of the extensive disagreement that was noted in [1] has disappeared in our new calculations.

4 $SO(3)$ and $SU(2)$

We turn now to $SO(3)$. A difference between $SO(3)$ and $SO(4)$ is that the fundamental flux tube in $SO(3)$ is visibly unstable [1], which is no surprise given that it corresponds to the adjoint flux tube of $SU(2)$. So extracting a string tension in $SO(3)$ is delicate and the result will not be very precise. Since we are interested in comparisons with $SU(2)$ that are precise enough to be significant, we will not consider the $SO(3)$ string tension any further in this paper.

We begin with the lightest glueball. In Table 4 we list our calculated values of the mass gap at various bare couplings. From these we can extract a continuum value for m_{0^+}/g^2 with the fit

$$\left. \frac{m_{0^+}}{g_I^2 N} \right|_{so3} = 0.1287(16) + 0.00098(41) a g_I^2 N \quad , \quad \chi^2/n_{dof} = 0.6 \quad (13)$$

as displayed in Fig. 4. Now for $SU(2)$ one finds $m_{0^+}/g^2|_{su2} = 1.5860(22)$. (See Table B1 of [5].) So if we assume that the mass gap is identical in $SU(2)$ and $SO(3)$, the above values of m_{0^+}/g^2 in $SO(3)$ and $SU(2)$ imply the following relationship between the couplings:

$$\frac{g_{so3}^2}{g_{su2}^2} = 4.108(51). \quad (14)$$

This should be compared to the theoretically expected value of 4 [1]. The agreement is within an acceptable 2σ . Alternatively we could assume this factor of 4 and then obtain a prediction for m_{0^+}/g^2 in $SU(2)$ which would be within about 2σ of the known value.

The continuum extrapolations in units of ag^2 suffer from their distance from the continuum limit, as is evident from Fig. 4. As in the case of $SO(4)$, a solution is to extrapolate ratios of physical masses. Since we do not have a usefully precise string tension to use in forming our dimensionless mass ratios we need to use some other quantity and we choose to use the mass gap since, being the lightest mass, it should also be the one that is calculated most accurately. So we extrapolate the ratio m_G/m_{0^+} with an $O(a^2 m_{0^+}^2)$ lattice correction for the various glueballs G , whose calculated masses are listed in Table 5. The resulting continuum values of these ratios are listed in Table 6 together with those for $SU(2)$ (and also, to be complete, those for $SO(4)$). The $SU(2)$ and $SO(3)$ mass ratios agree within $\sim 2\sigma$ for the 0^{+*} , the 0^{+***} , and the 0^{+****} , and also for the 2^+ , the 2^- , the 2^{+*} , the 2^{-*} . Of the remaining four glueballs only the 0^{+**} differs from the $SU(2)$ value by more than $\sim 3\sigma$. We note that just as in the case of $SO(4)$ all the significant differences are due to the $SO(3)$ mass estimates being larger than the $SU(2)$ ones, which is consistent with the systematic error incurred when extracting a mass too early in the correlator. The examples of effective mass plots in Fig. 2 show that while our new mass calculations involve operators that have a significantly better projection onto the various glueball states than the operators used in [1], they are not yet adequate for identifying unambiguously the effective mass plateaux of the heavier glueballs such as the 0^- and 1^\pm .

5 Conclusions

Our main motivation for the calculations in this paper was the apparent disagreement, observed in [1], between much of the low-lying spectrum of the $SO(4)$ gauge theory and that of $SU(2)$, and, to a lesser extent, that of $SO(3)$ as well. It was argued in [1] that this was probably due to the relatively poor overlap of the operators onto the corresponding glueball states. In this paper we improved the operators used and found much better agreement between the spectra of $SO(4)$, $SO(3)$ and $SU(2)$ gauge theories. The improvement has been greatest for $SO(4)$ where, for the lightest and most reliably calculated single particle states,

we now have agreement with $SU(2)$ and hence with the $SU(2) \times SU(2)$ theory with which $SO(4)$ shares its Lie algebra. And similarly for $SO(3)$ and $SU(2)$. We did not attempt to repeat the comparison between $SO(6)$ and $SU(4)$ because our operator improvement proved very modest for $SO(6)$ and in any case there was already reasonable agreement in [1] between the low-lying spectra of $SO(6)$ and $SU(4)$, except for a couple of scalar glueball excited states. So in summary all this points to the conclusion that the differing global properties of these $SO(N)$ and $SU(N')$ groups play no significant role in the low-lying physics of the corresponding gauge theories.

Acknowledgements

The numerical computations were carried out on the computing cluster in Oxford Theoretical Physics.

References

- [1] R. Lau and M. Teper, *SO(N) gauge theories in 2 + 1 dimensions: glueball spectra and confinement*, JHEP 1710 (2017) 022 [arXiv:1701.06941].
- [2] R. Lau and M. Teper, *The deconfining phase transition of SO(N) gauge theories in 2+1 dimensions*, JHEP 1603 (2016) 072 [arXiv:1510.07841].
- [3] G.P. Lepage and P.B. Mackenzie, *Viability of lattice perturbation theory*, Phys. Rev. D48 (1993) 2250 [arXiv:hep-lat/9209022].
G. Parisi, *Recent Progresses in Gauge Theories*, AIP Conf Proc 68 (1980).
- [4] M. Teper, *SU(N) gauge theories in 2+1 dimensions*, Phys.Rev. D59 (1999) 014512 [arXiv:hep-lat/9804008].
- [5] A. Athenodorou and M. Teper, *SU(N) gauge theories in 2+1 dimensions: glueball spectra and k-string tensions*, JHEP 1702 (2017) 015 [arXiv:1609.03873].
- [6] B. Lucini, M. Teper and U. Wenger, *Glueballs and k-strings in SU(N) gauge theories : calculations with improved operators*, JHEP 0406:012 (2004) [arXiv:hep-lat/0404008].

$L_s^2 L_t$	β	$\frac{1}{N}\text{tr}(U_p)$	am_P	$a\sqrt{\sigma}$	$\sqrt{\sigma/g^2 N}$
22 ² 32	11.0	0.8013472(21)	0.931(16)	0.2084(18)	0.05740(48)
26 ² 36	12.2	0.8229531(4)	0.8449(92)	0.1824(10)	0.05724(30)
30 ² 40	13.7	0.8440177(4)	0.7354(74)	0.1584(8)	0.05725(28)
34 ² 44	15.1	0.8595470(3)	0.6699(63)	0.1420(7)	0.05759(26)
38 ² 48	16.5	0.8722327(2)	0.6186(40)	0.1290(4)	0.05803(18)
42 ² 52	18.7	0.8880800(2)	0.5150(33)	0.1121(4)	0.05817(18)
46 ² 60	21.3	0.9023628(2)	0.4134(33)	0.0961(4)	0.05773(22)
–	∞	–	–	–	0.05889(41)

Table 1: $SO(4)$ average plaquette values, flux loop masses, and string tensions.

$L_s^2 L_t$	34 ² 42	42 ² 46	46 ² 52	50 ² 56	58 ² 62	66 ² 70	74 ² 80
β	11.0	12.2	13.7	15.1	16.5	18.7	21.3
0 ⁺	0.7040(59)	0.6118(58)	0.5325(44)	0.4788(46)	0.4301(37)	0.3722(33)	0.3526(26)
0 ⁺⁺	0.983(30)	0.902(19)	0.787(12)	0.671(36)	0.588(22)	0.522(15)	0.4672(87)
0 ⁺⁺⁺	1.243(19)	1.125(62)	0.961(27)	0.877(25)	0.784(12)	0.633(26)	0.595(20)
0 ⁺⁺⁺⁺	1.438(39)	1.27(11)	1.063(42)	0.892(58)	0.838(56)	0.760(20)	0.662(13)
0 ^{*****}	1.496(48)	1.318(26)	1.047(55)	0.962(36)	0.942(24)	0.792(32)	0.703(14)
2 ⁺	1.150(16)	1.027(13)	0.887(26)	0.795(16)	0.729(9)	0.619(12)	0.549(7)
2 ⁺⁺	1.432(55)	1.217(23)	1.070(41)	0.954(20)	0.868(18)	0.751(20)	0.652(14)
2 ⁻	1.147(23)	0.987(46)	0.868(18)	0.803(10)	0.732(13)	0.624(11)	0.522(11)
2 ^{-*}	1.375(47)	1.232(19)	1.106(19)	0.957(28)	0.881(17)	0.759(13)	0.655(12)
0 ⁻	1.519(62)	1.354(46)	1.089(62)	1.021(27)	0.925(26)	0.740(55)	0.689(38)
1 ⁺	1.73(11)	1.52(8)	1.124(59)	1.154(54)	1.028(37)	0.925(15)	0.812(25)
1 ⁻	1.71(9)	1.51(5)	1.30(11)	1.087(43)	1.033(30)	0.890(23)	0.792(23)

Table 2: $SO(4)$ glueball masses am_G .

$rM_G/\sqrt{\sigma}$			
J^P	$SO(4)$	χ^2/n_{dof}	$SU(2)$
0^+	4.735(40)	0.66	4.737(6)
0^{+*}	6.77(15)	1.70	6.861(14)
0^{+**}	8.64(19)	0.88	8.382(14)
0^{+***}	9.63(21)	0.55	9.278(16)
0^{+****}	10.23(23)	1.30	9.708(21)
2^+	8.06(11)	0.48	7.762(10)
2^-	7.93(14)	0.98	7.795(12)
2^{+*}	9.53(21)	0.13	9.107(20)
2^{-*}	9.69(18)	0.61	9.123(24)
0^-	9.86(38)	0.45	9.884(25)
1^+	11.87(33)	1.84	10.553(31)
1^-	11.24(33)	0.64	10.538(28)

Table 3: Continuum glueball masses in units of the string tension: the spectrum of $SO(4)$ gauge theory versus that of $SU(2)$, with $r = 1, \sqrt{2}$ for $SU(2), SO(4)$ respectively.

$L_s^2 L_t$	β	$\frac{1}{N}\text{tr}(U_p)$	am_{0^+}	$m_{0^+}/g^2 N$
$54^2 40$	6.5	0.8335239(13)	0.4391(21)	0.1322(7)
$62^2 48$	7.0	0.84655214(20)	0.4004(21)	0.1318(7)
$74^2 60$	8.5	0.87556397(12)	0.3161(14)	0.1307(6)
$82^2 64$	9.0	0.88291502(10)	0.2952(21)	0.1303(10)
$90^2 70$	10.0	0.89526817(7)	0.2647(17)	0.1317(9)
$100^2 80$	11.0	0.90524861(6)	0.2361(17)	0.1306(10)
—	∞	—	—	0.1287(16)

Table 4: $SO(3)$ average plaquette values, the mass gap and its continuum extrapolation.

$L_s^2 L_t$	54 ² 40	62 ² 48	74 ² 60	82 ² 64	90 ² 70	100 ² 80
β	6.5	7.0	8.5	9.0	10.0	11.0
0 ⁺	0.4391(21)	0.4004(21)	0.3161(14)	0.2952(21)	0.2647(17)	0.2361(17)
0 ^{+*}	0.6461(76)	0.5786(44)	0.4637(37)	0.4384(38)	0.3890(40)	0.3438(38)
0 ^{+**}	0.766(13)	0.732(9)	0.576(11)	0.542(8)	0.4908(49)	0.4287(86)
0 ^{+***}	0.848(18)	0.773(13)	0.617(15)	0.601(10)	0.533(13)	0.4655(93)
0 ^{+****}	0.883(21)	0.833(20)	0.642(14)	0.592(23)	0.559(14)	0.497(17)
2 ⁺	0.707(18)	0.645(17)	0.520(6)	0.4890(72)	0.4320(51)	0.3875(52)
2 ^{+*}	0.882(22)	0.790(15)	0.6364(67)	0.581(12)	0.5218(67)	0.4725(55)
2 ⁻	0.726(10)	0.661(9)	0.5200(58)	0.4945(49)	0.4351(49)	0.3945(42)
2 ^{-*}	0.872(25)	0.758(32)	0.626(12)	0.5871(86)	0.507(10)	0.4684(76)
0 ⁻	0.920(22)	0.858(15)	0.7086(89)	0.651(12)	0.554(15)	0.476(18)
1 ⁺	0.944(48)	0.937(23)	0.787(27)	0.704(19)	0.595(21)	0.556(8)
1 ⁻	1.011(43)	0.932(27)	0.753(27)	0.738(22)	0.630(25)	0.546(13)

Table 5: $SO(3)$ glueball masses am_G .

J^P	M_G/M_{0^+}				
	$SO(3)$	χ^2/n_{dof}	$SO(4)$	χ^2/n_{dof}	$SU(2)$
0 ^{+*}	1.476(18)	0.89	1.424(32)	1.37	1.449(4)
0 ^{+**}	1.882(30)	1.01	1.832(40)	0.66	1.770(4)
0 ^{+***}	2.042(43)	0.76	2.024(47)	0.48	1.959(4)
0 ^{+****}	2.105(60)	0.61	2.149(51)	1.29	2.050(5)
2 ⁺	1.659(29)	0.25	1.700(24)	0.33	1.639(3)
2 ⁻	1.665(22)	0.47	1.675(30)	1.19	1.646(3)
2 ^{+*}	1.991(34)	0.54	2.009(45)	0.10	1.923(5)
2 ^{-*}	1.969(43)	0.85	2.050(38)	0.65	1.926(6)
0 ⁻	2.219(53)	3.46	2.085(80)	0.43	2.087(6)
1 ⁺	2.391(57)	1.78	2.515(80)	1.81	2.228(7)
1 ⁻	2.393(74)	1.12	2.378(70)	0.56	2.225(7)

Table 6: Continuum glueball masses in units of the mass gap: comparing the spectra of $SO(3)$ and $SO(4)$ gauge theories with that of $SU(2)$.

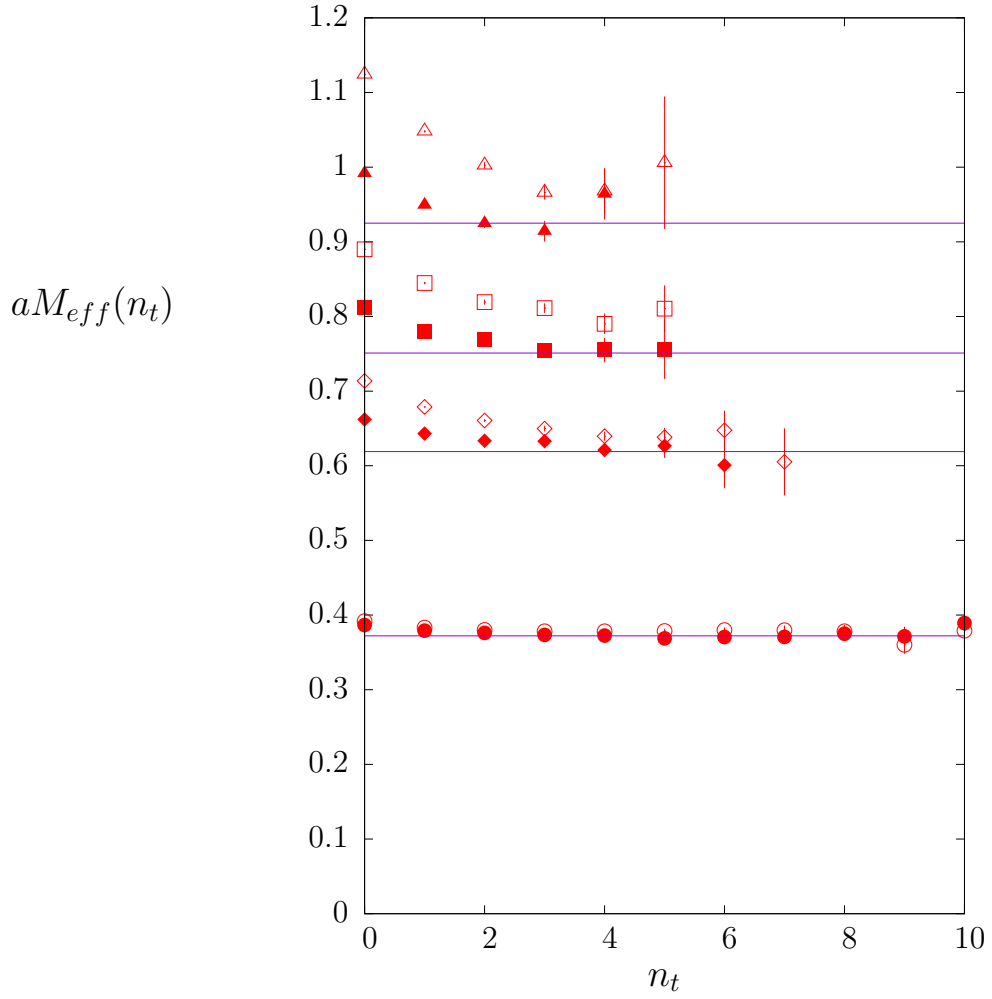


Figure 1: Some effective masses in $SO(4)$ at $\beta = 18.7$. Solid points are new calculations while open points are from the older calculations in [1]. Glueballs shown are lightest $J^P = 0^+$ (circles), lightest 2^+ (diamonds), first excited 2^+ (boxes), and lightest 1^+ (triangles). Horizontal lines are our corresponding mass estimates as listed in Table 2.

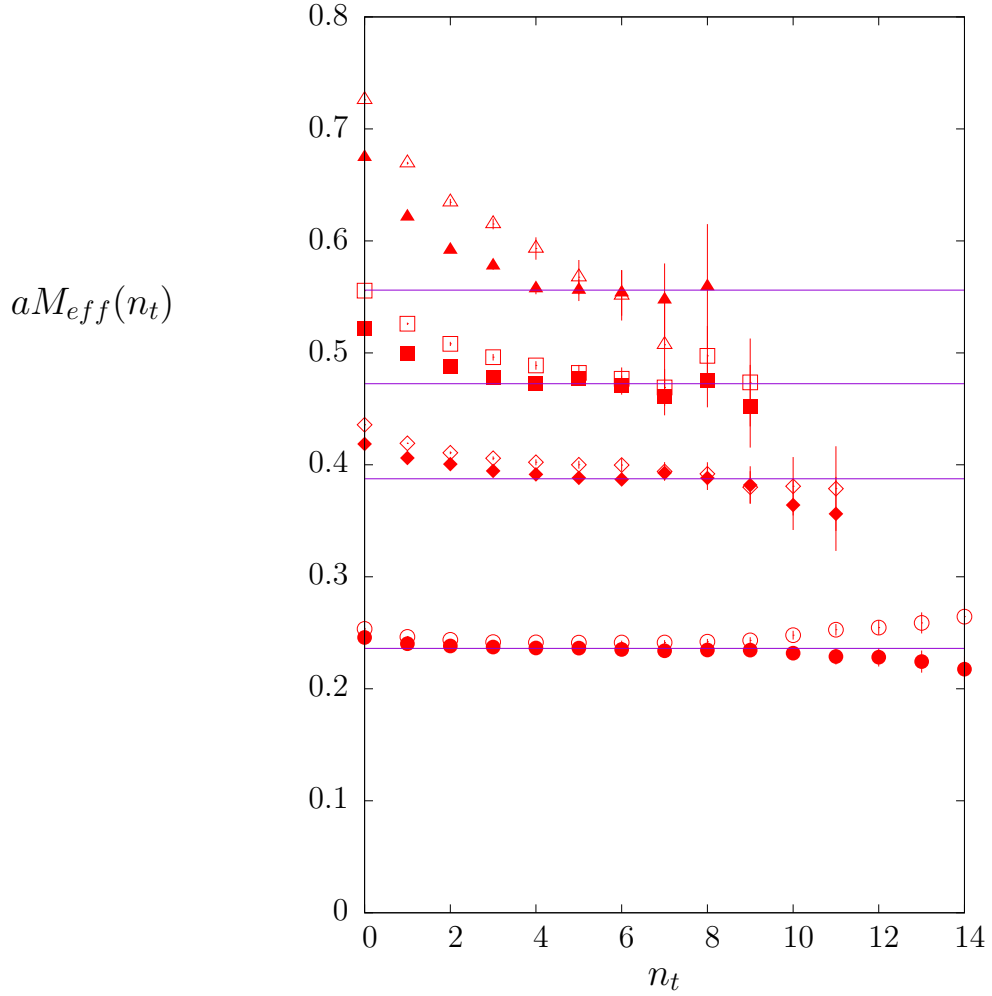


Figure 2: Some effective masses in $SO(3)$ at $\beta = 11.0$. Solid points are new calculations while open points are from the older calculations in [1]. Glueballs shown are lightest $J^P = 0^+$ (circles), lightest 2^+ (diamonds), first excited 2^+ (boxes), and lightest 1^+ (triangles). Horizontal lines are our corresponding mass estimates as listed in Table 5.

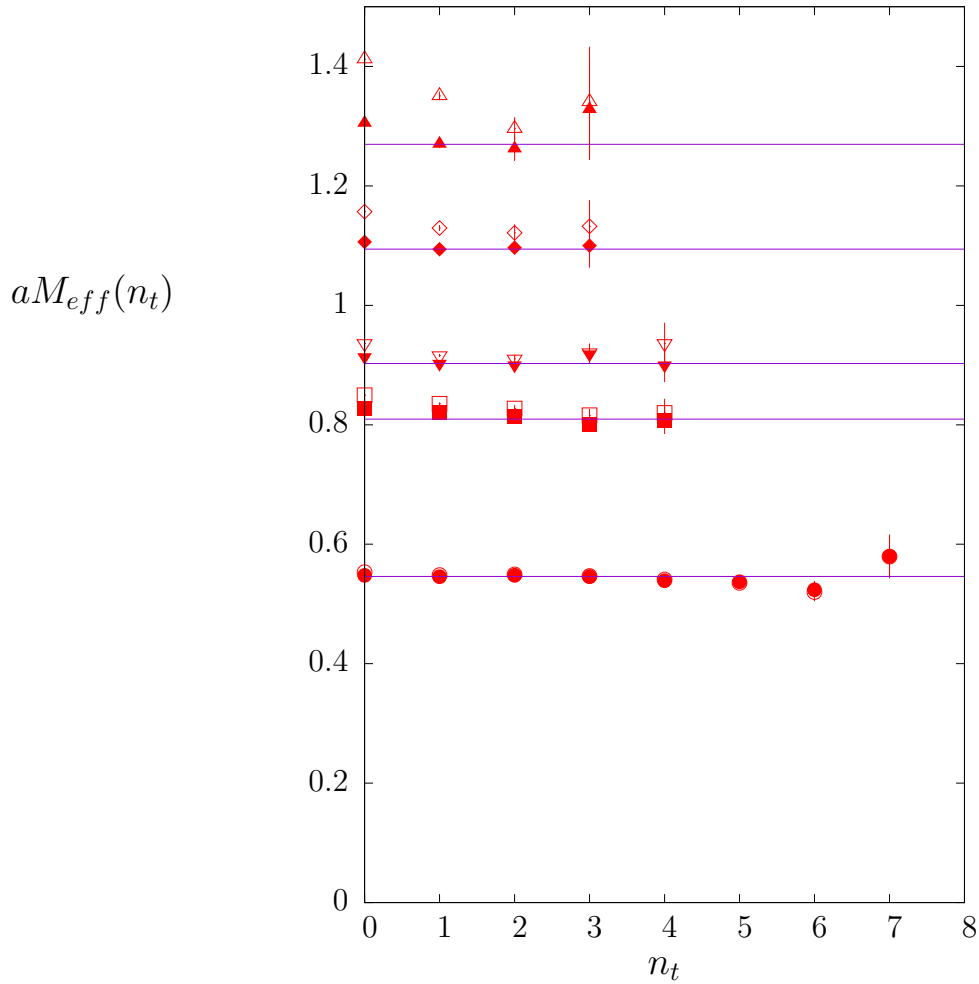


Figure 3: Some glueball effective masses in $SU(4)$ at $\beta = 51.0$. Solid points are from operators in fundamental representation and open points in $k = 2$ antisymmetric representation. Glueballs shown are lightest $J^P = 0^+$ (circles), first excited 0^+ (boxes), lightest 2^+ (inverted triangles), first excited 2^+ (diamonds), and lightest 1^+ (triangles). Horizontal lines are the corresponding asymptotic mass estimates using operators in fundamental representation.

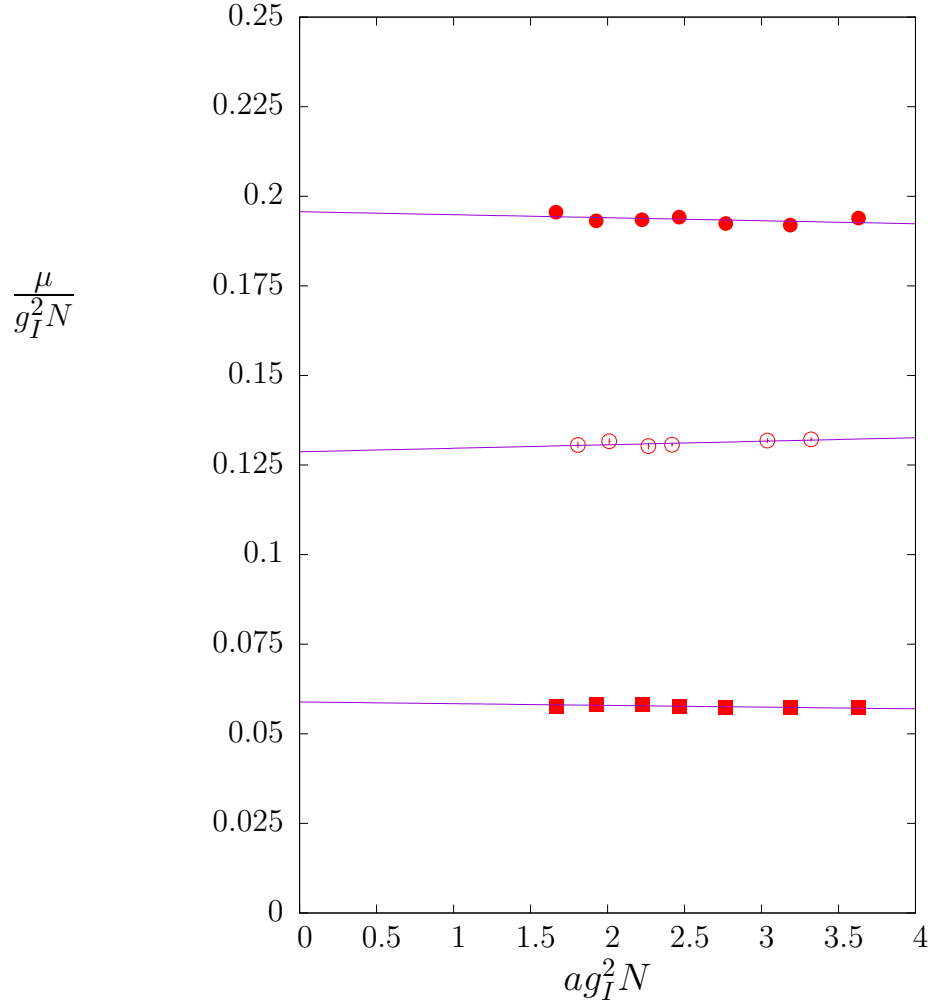


Figure 4: Some continuum masses in units of the lattice 't Hooft coupling, with linear extrapolations to the continuum limit : for $\mu = M_{0+}$ in $SO(4)$ (\bullet) and in $SO(3)$ (\circ), and for $\mu = \sqrt{\sigma_f}$ in $SO(4)$ (\blacksquare).

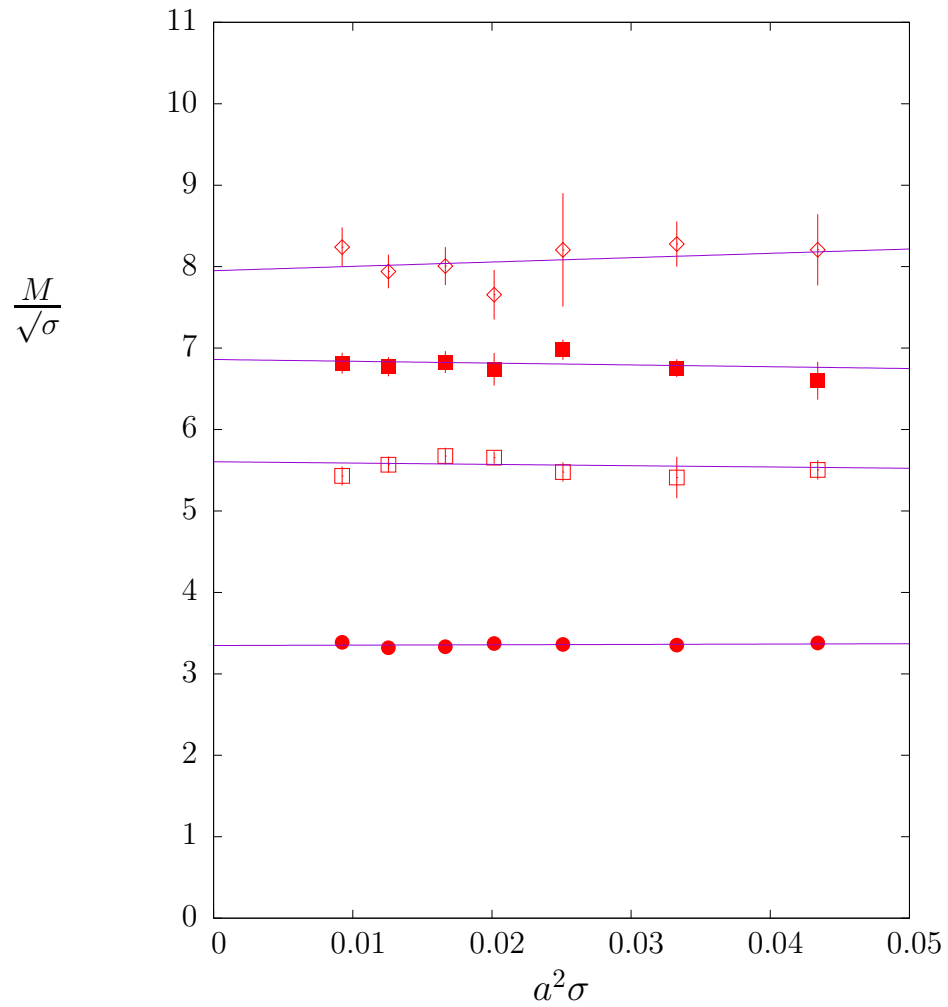


Figure 5: Some masses in units of the string tension in $SO(4)$, with linear extrapolations to the continuum limit : for $M = M_{0+}$ (\bullet), $M = M_{2-}$ (\circ), $M = M_{2^*}$ (\blacksquare), and $M = M_{1-}$ (\diamond).